Human Cell
https://doi.org/10.1007/s13577-024-01121-7

RESEARCH ARTICLE

Sequencing-based study of neural induction of human dental pulp stem cells

Shohei Takaoka[1,2] · Fumihiko Uchida[3] · Hiroshi Ishikawa[2,4] · Junko Toyomura[2,4] · Akihiro Ohyama[2,4] · Hideaki Matsumura[2,4] · Koji Hirata[2,4] · Satoshi Fukuzawa[1] · Naomi Ishibashi Kanno[3] · Aiki Marushima[2,4] · Kenji Yamagata[3] · Toru Yanagawa[3] · Yuji Matsumaru[2,4] · Eiichi Ishikawa[2,4] · Hiroki Bukawa[3]

Received: 13 June 2024 / Accepted: 11 August 2024

Abstract

Techniques for triggering neural differentiation of embryonic and induced pluripotent stem cells into neural stem cells and neurons have been established. However, neural induction of mesenchymal stem cells, including dental pulp stem cells (DPSCs), has been assessed primarily based on neural-related gene regulation, and detailed studies into the characteristics and differentiation status of cells are lacking. Therefore, this study was aimed at evaluating the cellular components and differentiation pathways of neural lineage cells obtained via neural induction of human DPSCs. Human DPSCs were induced to neural cells in monolayer culture and examined for gene expression and mechanisms underlying differentiation using microarray-based ingenuity pathway analysis. In addition, the neural lineage cells were subjected to single-cell RNA sequencing (scRNA-seq) to classify cell populations based on gene expression profiles and to elucidate their differentiation pathways. Ingenuity pathway analysis revealed that genes exhibiting marked overexpression, post-neuronal induction, such as *FABP7* and *ZIC1*, were associated with neurogenesis. Furthermore, in canonical pathway analysis, axon guidance signals demonstrated maximum activation. The scRNA-seq and cell type annotations revealed the presence of neural progenitor cells, astrocytes, neurons, and a small number of non-neural lineage cells. Moreover, trajectory and pseudotime analyses demonstrated that the neural progenitor cells initially engendered neurons, which subsequently differentiated into astrocytes. This result indicates that the aforementioned neural induction strategy generated neural stem/progenitor cells from DPSCs, which might differentiate and proliferate to constitute neural lineage cells. Therefore, neural induction of DPSCs may present an alternative approach to pluripotent stem cell-based therapeutic interventions for nervous system disorders.

Keywords Mesenchymal stem cells · Neural stem cells · Neurons · Astrocytes · Neural induction

Introduction

Neural stem cells (NSCs) are essential in the central nervous system during neurogenesis, which occurs throughout embryonic development and adulthood [1]. NSCs are capable of self-renewal and progenitor cell-mediated differentiation into neurons, astrocytes, and oligodendrocytes. This property facilitates the in vitro culture of NSCs, making them extremely attractive for investigating neurogenesis and progenitor-mediated development of various cell lineages. Moreover, NSC transplantation is assumed to exert therapeutic effects in neurodegenerative disorders, cerebrovascular diseases, and traumatic brain or spinal cord injuries via regeneration, repair, or enhancement of central nervous system functions [2–5]. NSCs also substantially contribute

✉ Fumihiko Uchida
f-uchida@md.tsukuba.ac.jp

1 Department of Oral and Maxillofacial Surgery, University of Tsukuba Hospital, Tsukuba, Ibaraki, Japan

2 Laboratory of Clinical Regenerative Medicine, Department of Neurosurgery, Faculty of Medicine, University of Tsukuba, Tsukuba, Ibaraki, Japan

3 Department of Oral and Maxillofacial Surgery, Institute of Medicine, University of Tsukuba, Tsukuba, Ibaraki, Japan

4 Department of Neurosurgery, Institute of Medicine, University of Tsukuba, Tsukuba, Ibaraki, Japan

Published online: 29 August 2024

to the establishment of disease models and drug and toxicity screening research [6].

Pluripotent stem cells, such as embryonic stem cells (ESCs) and induced pluripotent stem cells (iPSCs), can generate NSCs in vitro. Recently, several protocols, comprising monolayer culture, neural rosettes, and three-dimensional aggregate organoids, have been established for the neural induction of pluripotent stem cells [6–9]. NSC-derived neural lineage cells have been meticulously characterized by their gene expression profiles, and differentiated cells have been compared with cells in vivo [10–12]. However, the risk of tumorigenesis in iPSCs and ethical concerns associated with ESCs warrant the identification of alternative sources of pluripotent stem cells for clinical application.

Mesenchymal stem cells (MSCs), a class of multipotent stem cells, have the potential to differentiate into mesodermal cell lineages, namely chondrocytes, osteocytes, and adipocytes, as well as into ectoderm- or endoderm-derived neural lineage cells and hepatocytes [13–15]. MSCs predominantly manifest an intrinsic expression profile encompassing a diverse array of NSC markers, including nestin, alongside neuron-specific markers, such as doublecortin and β3-tubulin, thereby establishing their neurogenic propensity [16–18]. Notably, dental pulp stem cells (DPSCs) exhibit high neurogenic capabilities, as evidenced by their augmented expression of NSC- and neuron-specific markers compared with that in other MSCs because of their origin from neural crest cells [18, 19]. For these reasons, DPSCs are considered an optimal reservoir for neural induction of MSCs. Nonetheless, it is challenging to evaluate the efficacy of neural induction with the inherent expression of these neural markers in MSCs, including DPSCs, rendering the comprehensive characterization of cells post-neuronal induction elusive. The neural induction of DPSCs has also been primarily evaluated by increased expression of neural markers [19–21]; however, the differentiation status of the cells has not been identified.

This study was aimed at investigating neural induction of human DPSCs and the associated gene expression profile using single-cell RNA sequencing (scRNA-seq) and microarray-based ingenuity pathway analysis (IPA). This study was also aimed at delineating neural lineage cells originating from human DPSCs by conducting a thorough assessment of gene expression profiles at the single-cell level and categorizing them within the established cell type dataset. The results of this study demonstrate that our neural induction protocol yields neural lineage cells, including neural progenitors, astrocytes, and neurons, along with a limited number of non-neural lineage cells from human DPSCs.

Materials and methods

Isolation and culture of DPSCs

This study was approved by the University of Tsukuba Clinical Research Ethics Review Committee (Approval Number: H29-173), and informed consent was obtained from the study participants. For isolation and culture of DPSCs, cell culture dishes, surface-treated with gas plasma, were used. DPSCs were isolated following a previously described methodology [2, 22]. Dental pulp tissue was acquired from teeth extracted from healthy patients at the Department of Oral and Maxillofacial Surgery, University of Tsukuba Hospital, sectioned into diminutive fragments, and subjected to static cultivation to procure migrating cells from each fragment. Subsequently, 1×10^3 single cells were inoculated into 10 cm cell culture dishes (Falcon Standard Tissue Culture Dishes; Corning, Corning, NY, USA) and cultured for approximately 10 days. The colonies exhibiting maximum proliferation were identified and used as DPSCs in subsequent experiments. The culture was sustained in Dulbecco's modified Eagle's medium/Ham's nutrient mixture F12 (DMEM/F12; Thermo Fisher Scientific, Waltham, MA, USA), fortified with 10% fetal bovine serum (FBS; Sigma-Aldrich Corporation, St. Louis, MO, USA), 100 µM glutamate (GlutaMAX I; Thermo Fisher Scientific), 0.1% MEM non-essential amino acids (MEM-NEAA; Thermo Fisher Scientific), 50 U/mL penicillin and 50 µg/mL streptomycin (both from Fujifilm Wako Pure Chemicals Corporation, Tokyo, Japan), and 0.25 µg/mL fungizone (Cytiva, Marlborough, MA, USA), and incubated at 37 °C in the presence of 4.7% CO_2. The DPSCs were passaged and perpetuated at 1:3 ratio.

Neural induction of DPSCs

DPSCs were induced to differentiate into neural cells following the methodology outlined by Takahashi et al. [23]. DPSCs were aliquoted (1×10^4) into 60 mm culture dishes, and neural induction was performed for approximately 2 weeks. The neural induction medium comprised DMEM/F12, supplemented with 5% FBS, 10 mM MEM-NEAAs, 10 nM all-trans retinoic acid (Sigma-Aldrich), 2 mM glutamate (Sigma-Aldrich), 50 mM ascorbic acid (Sigma-Aldrich), 5 mM insulin (Sigma-Aldrich), 10 nM dexamethasone (Sigma-Aldrich), 20 nM progesterone (Sigma-Aldrich), 20 nM estradiol (Sigma-Aldrich), 10 nM neural growth factor-1 (Sigma-Aldrich), 10 ng/mL thyroxine (Sigma-Aldrich), 50 U/mL penicillin, and 50 µg/mL streptomycin. Distinctive colonies exhibiting

morphological divergence from the surrounding DPSCs were identified under a phase-contrast microscope and retrieved using filter paper soaked in a solution containing 0.1% trypsin and 0.02% EDTA/phosphate-buffered saline (−). The harvested colonies were subsequently cultured in a neurobasal medium supplemented with B27 (Thermo Fisher Scientific), 20 µg/mL basic fibroblast growth factor (PeproTech, Cranberry, PA, USA), and 20 µg/mL epidermal growth factor (PeproTech), and sustained in cell culture dishes coated with BD Matrigel® Basement Membrane (BD Biosciences, San Jose, CA, USA). The cell cultures were maintained under controlled environmental conditions at 37 °C and 4.7% CO_2. The nervous system cells were passaged at 1:3 ratio and defined as neural-induced DPSCs (Ni-DPSCs).

Microarray-dependent *IPA*

DPSCs procured from the teeth of three participants and individual DPSC-derived Ni-DPSCs were subjected to comprehensive genetic analyses using the Human Clariom S Assay (Thermo Fisher Scientific). Data on these cell populations were processed using the Expression Console 1.3.1 software (Thermo Fisher Scientific). Quality control assessment was conducted using the Transcriptome Analysis Console software version 3.1.0.5 (Thermo Fisher Scientific). The data were used to enlist biological functions in the Ingenuity KnowledgeBase and are publicly available in the Gene Expression Omnibus (GEO; Accession Number: GSE168399). Fluctuations in gene expression were recorded, and the values were entered into the IPA software version 01-20-04 (QIAGEN, Hilden, Germany) for analyses. Upstream regulator analysis was used to predict upstream molecules, which may be causing the observed changes in gene expression. A causal network analysis was performed to identify the master regulatory factors presumably implicated in the observed alterations in gene expression. This analysis allows for the discovery of novel regulatory mechanisms by including regulatory factors, not directly related to the targets in the data set, in the prediction**.** The z-score was used to predict the activation status of the canonical pathway.

Library preparation and scRNA-seq

Ni-DPSCs cultured for 2 days in vitro (DIV) were used in the experiment. The adherent cells were dissociated using trypsin, and following singlet processing, they were filtered using a 40 µm cell strainer. The cells were stained with trypan blue and observed under a microscope to assess cell counts and viability; single-cell suspensions with viability > 80% were employed for library preparation. Single-cell libraries were engineered in accordance with the 10 × Genomics protocol (Chromium Next GEM Single Cell 3′ Reagent Kits v3.1; Dual Index; CG000315 Rev E) and sequenced using NovaSeq 6000 (Illumina Inc., San Diego, CA, USA). The data are publicly available in GEO (Accession Number: GSE272111).

Analysis of scRNA-seq data

Cell Ranger (Version 7.1.0, 10 × Genomics, Pleasanton, CA, USA) was used to perform unique molecular identifier (UMI) quantification, adhering to the default and recommended parameters to fashion a filtered gene-barcode matrix for each sample. Low-quality cells (number of UMIs < 10,000 and percentage of mitochondrial reads > 20%) were screened using Seurat version 4.2.1 (R software). Doublet cells were detected and eliminated from the analysis based on the parameters recommended by DoubletFinder (R software). UMI counts were normalized and scaled using the "logNormalize" method in the NormalizeData function. The nonlinear dimension was reduced using RunUMAP with principal components. The unique characteristics of each individual cell community and cluster were discerned using the FindNeighbors and FindClusters functions in Seurat (R software). Differentially expressed gene markers in each cluster were identified using the FindAllMarkers function in Seurat (R software). To annotate all cell clusters, the marker genes of each cluster and cell types were compared using CellMarker 2.0 and SCSA (Version 1.0), respectively. Trajectory and pseudotime analyses were performed using STREAM (Version 1.0), wherein the state of the cell at the branching and endpoints of cell differentiation is indicated by S [number].

Immunofluorescence staining

Please refer to the Supplementary Information for a detailed account of this procedure.

Results

Morphological evaluation of Ni-DPSCs

The DPSCs were spindle shaped and morphologically similar to fibroblasts (Fig. 1a). Ni-DPSCs at 2 DIV, composed of cells with various morphologies, both large and small, were obtained after neural induction (Fig. 1b). The Ni-DPSCs comprised numerous cell layers, with minute cells in the top layer at 2 and 5 DIV (Fig. 1c).

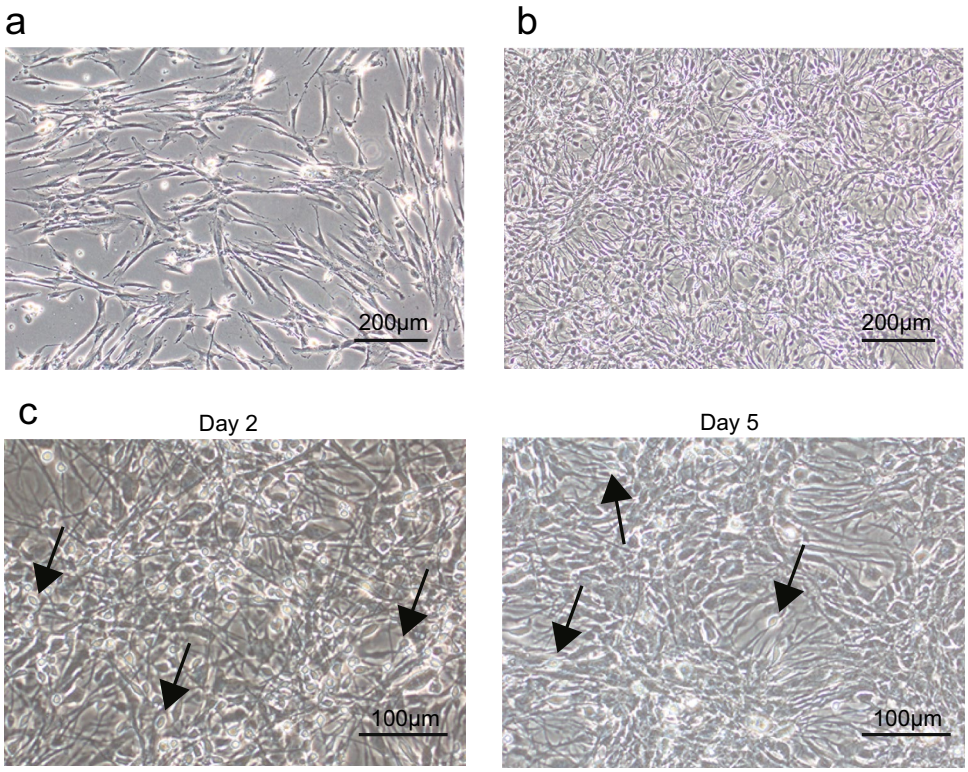

Fig. 1 Morphology of neural-induced dental pulp stem cells (Ni-DPSCs). **a** Phase-contrast micrograph of DPSCs. **b** Phase-contrast micrograph of Ni-DPSCs at 2 DIV. **c** High-magnification phase-contrast micrographs of Ni-DPSCs at 2 and 5 DIV. Many small cells are observed in the top layer (black arrows)

Comparison between genes expressed in DPSCs and Ni-DPSCs using *IPA*

Ni-DPSCs at 2 DIV were used in the experiment. Compared with DPSCs, the most upregulated gene in Ni-DPSCs was the NSC and astrocyte marker *FABP7* [24, 25]. In addition, the expression of the astrocytic marker *S100B*, and *ZIC1*, a prominent regulator of neurogenesis [26, 27], was considerably enhanced (Fig. 2a). Regarding molecular and cellular functions, proliferation, organization, and development during neural induction were noted. Neurodevelopment was demonstrated in physiological system development and function. Embryonic development was also observed (Fig. 2b). During the differentiation of DPSCs into Ni-DPSCs, beta-estradiol (important for embryonic and neural development), KRAS (important for cell proliferation), TGFB1, dexamethasone, and TNF were speculated to function as upstream regulators (Fig. 2c). Furthermore, causal network analysis, an extension of the upstream regulator analysis, was performed to predict the master regulator. Beta-estradiol and SOX2, which are important for maintaining stemness in NSCs, were predicted to be the master regulators. Furthermore, ACTL6A, essential for the proliferation of neural progenitor cells, was also predicted as a master regulator (Fig. 2d). It is unclear how PFDN5, a repressor of MYC transcriptional activity, and HEXIM1, a transcriptional inhibitor of RNA polymerase II, are involved in this neural induction. Among the top five master regulators, SOX2 and HEXIM1 were the predicted inhibitors. The canonical pathway analysis predicted that axon guidance signaling was the most prominent signal (Fig. 2e).

Identification of Ni-DPSC subpopulations and gene expression signatures

To assess the diversity of Ni-DPSCs at 2 DIV, scRNA-seq was performed in accordance with the 10 × Genomics transcriptomic protocol. The 13 clusters identified based on the expression of genes across a population of 7193 cells were visualized using uniform manifold approximation and projection (UMAP), and five cell populations—neural progenitor cells, astrocytes, neurons, epithelial cells/smooth muscle cells, and fibroblasts/mesenchymal cells—were identified according to the expression matrix of the marker genes (Fig. 3a). The population of each cluster comprised approximately 42% neural progenitor cells, 31% astrocytes, 11% epithelial and/or smooth muscle cells, 9% fibroblasts and/or mesenchymal cells, and 7% neurons (Fig. 3b). Based on the differential gene expression analysis, a heat map was generated using the top 10 marker genes for each identified cluster (Fig. 3c, Supplementary Table 1). The top two expressed genes in each cluster are shown in UMAP (Supplementary Fig. 1). Many genes were expressed across these clusters. *GFAP* is a gene characteristic of two astrocyte clusters (astrocytes 1 and 3).

a

TOP10 Upregulated genes	TOP10 Downregulated genes
FABP7	*COL6A3*
ZIC1	*COL12A1*
A2M	*GREM1*
SLC35F1	*LUM*
ISLR	*MASP1*
RTN1	*MAFP4*
PTPRZ1	*MME*
HLA-DRA	*ASPN*
S100B	*BGN*
PARM1	*TBX3*

b

Molecular and Cellular Functions	Molecules	*p*-Value
Cellular Assembly and Organization	1381	1.91E-14 - 1.91-E83
Cellular Function and Maintenance	1607	1.91E-14 - 1.91-E83
Cellular Development	2102	9.37E-15 - 1.91-E73
Cellular Growth and Proliferation	1962	4.20E-15 - 1.91-E73
Cell Morphology	1167	1.52E-14 - 1.91-E70

Physiological System Development and Function	Molecules	*p*-Value
Organismal Survival	1491	4.35E-16 - 4.66E-89
Nervous system Development and Function	1321	6.56E-15 - 1.32E-73
Organism Development	2135	2.38E-14 - 1.32E-73
Tissue Development	1882	2.01E-14 - 1.32E-73
Embryonic Development	1571	2.38E-14 - 2.01E-63

c

Predictid Activation: Inhibited

Upstream Regulator	*p*-Value
beta-estradiol	4.55E-99
TGFB1	5.25E-89
dexamethasone	7.23E-81
KRAS	3.79E-64
TNF	1.79E-63

d

Predictid Activation: Inhibited

Predicted Master Regulator	*p*-Value
beta-estradiol	4.80E-118
PFDN5	8.82E-116
SOX2	9.04E-114
ACTL6A	6.66E-111
HEXIM1	2.39E-110

e

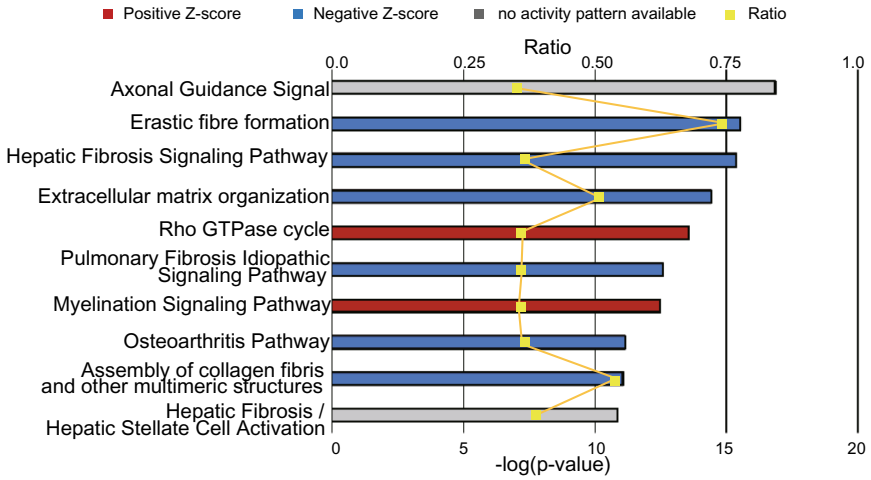

Fig. 2 IPA analysis of DPSCs vs. Ni-DPSCs. **a** Top 10 upregulated and downregulated genes between Ni-DPSCs and DPSCs. **b** Top five biological, molecular, and cellular functions, and physiological system development and functions identified through the Ingenuity pathway analysis (IPA). **c** Top five regulators that predict upstream molecules, which may have caused the observed changes in gene expression, predicted using the upstream regulator analysis of IPA. Factors predicted to behave as inhibitors are shown in red. **d** Top five predicted master regulators that control the expression of genes in our datasets, identified through the causal network analysis of IPA. Factors predicted to behave as inhibitors are shown in red. **e** Top 10 canonical pathways, identified using IPA. "Ratio" is the number of differentially expressed genes that fit into each pathway relative to the overall number of genes in that pathway

Trajectory and pseudotime analyses of Ni-DPSCs

Before performing trajectory and pseudotime analyses, Ni-DPSC clusters were broadly classified into astrocytes, neural progenitor cells, neurons, and non-neuronal cells (Fig. 4a). To assess the differentiation into increasingly specialized cell subtypes, a trajectory analysis was performed (Fig. 4b). S1–S3, S5–S7, and S13 were the branching points for cell differentiation. The differentiation pathways of neural progenitor cells, astrocytes, and non-neural lineage cells were S0–S12, whereas S13–S15 were inferred as the differentiation pathways of neurons from neural progenitor cells. Flat tree and subway map plots revealed that neural progenitor cells could be divided into three groups—those that differentiate into neurons, those that remain neural progenitors, and those that differentiate into astrocytes, which were found to differentiate first into neurons (S7) and then into astrocytes (S3). In the final stage of differentiation, astrocytes transformed into non-neural lineage cells (Fig. 4c, d). Astrocytes and neural progenitor cells changed into clusters as differentiation progressed, indicating that these multiple clusters could be classified according to the degree of differentiation (Fig. 4d).

Assessment of neural-related marker proteins in cultured Ni-DPSCs

Ni-DPSCs at 2 DIV were characterized via immunocytochemical staining (Fig. 5a). In many Ni-DPSCs, the NSC

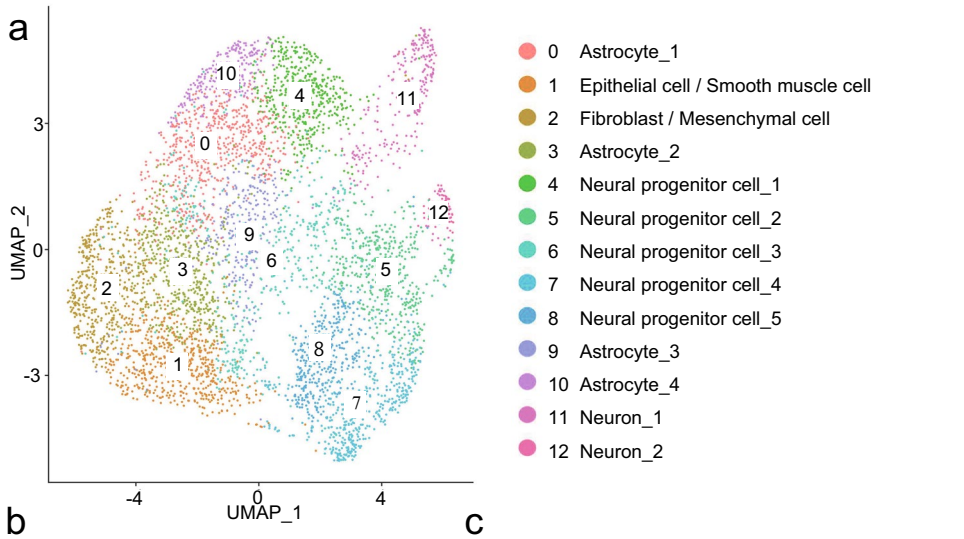

Cluster		Population (%)
0	Astrocyte_1	11.6
1	Epithelial cell / Smooth muscle cell	11.0
2	Fibroblast / Mesenchymal cell	9.2
3	Astrocyte_2	9.1
4	Neural progenitor cell_1	8.9
5	Neural progenitor cell_2	8.6
6	Neural progenitor cell_3	8.5
7	Neural progenitor cell_4	8.5
8	Neural progenitor cell_5	7.2
9	Astrocyte_3	5.4
10	Astrocyte_4	5.3
11	Neuron_1	5.3
12	Neuron_2	1.4

Fig. 3 Single-cell RNA sequencing analysis of Ni-DPSCs. **a** Two-dimensional UMAP depicting single cells, colored to represent 13 different transcriptionally distinct clusters. **b** Population of each cluster; total is shown as 100%. **c** Gene expression heatmap of the top 10 characteristic genes for each cluster

markers, nestin, FABP7, and SOX2, as well as the glial cell marker GFAP, were expressed. Ki-67 was expressed in the nuclei of many cells, indicating active cell proliferation. However, the cells with small nuclei did not express Ki-67. The GFAP-positive cells were the neuronal progenitor cell marker DCX-positive cells at 2 DIV. Cells positive for αSMA, a mesenchymal marker for smooth muscle cells, as well as fibroblasts were present. Neuronal maturation was indicated by the expression of synaptophysin, which is indicative of presynaptic vesicles, and neurite elongation (Fig. 5b). Synaptophysin-positive neurons were observed at 10 DIV but not at 5 DIV.

Discussion

Our neural induction protocol generated neural progenitor cells from human DPSCs and further demonstrated that neural progenitor cells differentiated into neurons and astrocytes. Among adult stem cells, MSCs are stromal cells capable of self-renewal and differentiation into various cell types, and their use is free of ethical concerns, teratoma development, and histocompatibility issues [28]. Furthermore, MSCs are attractive research targets because of their ease of extraction, isolation, and maintenance. Therefore, neural induction of MSCs has been widely attempted. Many neural-related marker genes and proteins are expressed or their expression increases when cultured under certain conditions [16, 17, 29–32]. The commonly used neural-related markers are the NSC markers (nestin and SOX2), neural markers (β3-tubulin and NF200), and glial marker (GFAP). Recently, Gao et al. [28] reported on the induction of adipose stem cells toward neurons. This induction results in increased expression of neuron-associated proteins and electrophysiological activity. However, the morphology and localization of synaptic vesicles are not characteristic of neurons, suggesting that they may differentiate into neurons.

Karakaş et al. [33] reported the induction of bone marrow stem cell toward neurons. The induced cells were assessed for morphological changes, increases or decreases in neuro-related markers, and electrophysiological activity. Furthermore, the induction of NSCs and oligodendrocytes from the MSCs of the human umbilical cord and placenta has been reported; however, only the expression of neuron-related markers and their increase or decrease were evaluated [34]. Thus, neural induction of MSCs is primarily assessed by

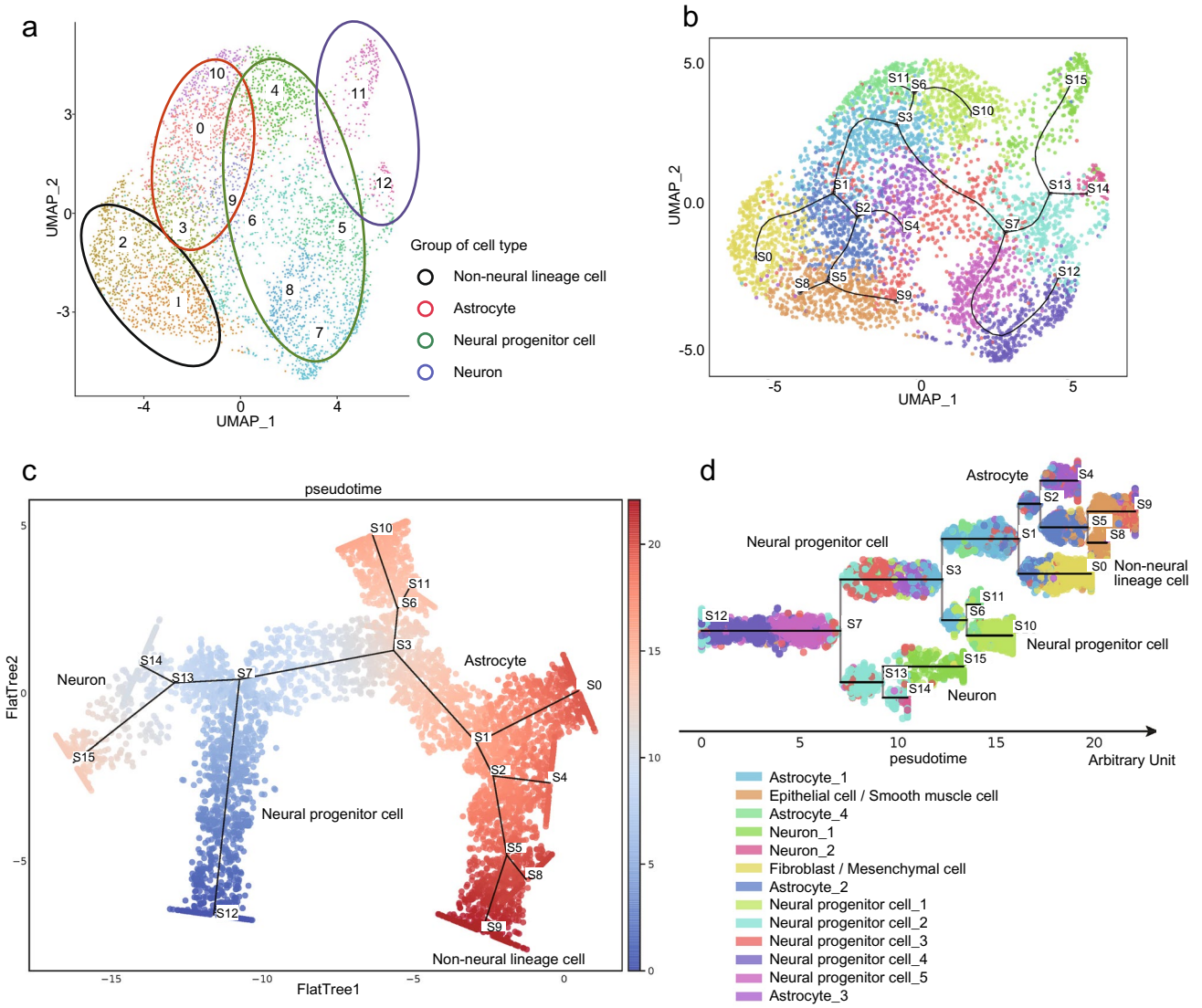

Fig. 4 Trajectory inference and pseudotime analysis. **a** The 13 clusters are divided into four groups: non-neural lineage cell, astrocyte, neural progenitor cell, and neuron. **b** Trajectory inference for all single cells throughout differentiation revealed five branches (S1, 2, 3, 6, and 13). **c** Pseudotime flat tree map of each subpopulation generated by STREAM. From the blue plot to the red plot, the cellular hierarchy by pseudotime trajectory is shown. **d** Pathways of cell differentiation by pseudotime trajectories are shown for 13 clusters

the expression of neuron-related genes or proteins and by their increase or decrease. However, MSCs are a heterozygous cell population, and there are many cells that originally express nestin as NSC markers, β3 tubulin as neuronal markers, and glial cell markers, such as GFAP and A2B5 [16–18]. In addition, MSCs exhibit electrical activity [35]. Therefore, it is difficult to accurately determine the results of MSC neural induction.

Gancheva et al. [36] collected RNA from whole cultured cells after neural induction of DPSCs and performed transcriptomic and bioinformatic analyses. After neural induction, cell type was restricted to the neuronal lineage but the stages of cell differentiation were not observed. To accurately assess the characteristics and differentiation status of a cell, it is necessary to comprehensively evaluate gene expression in single cells. scRNA-seq is an approach used to elucidate RNA transcripts in individual cells and to unravel the composition of different cell types and functions in highly complex tissues and cultured cells [37]. In the present study, single-cell analysis was used to accurately evaluate the results of neural induction of DPSCs.

Progenitor cells are intermediates between stem cells and differentiated cells; however, it is difficult to accurately distinguish multipotent NSCs from neural progenitors. In fact, differentiated cells do not differentiate directly from NSCs but differentiate through the progenitor cell stage [38].

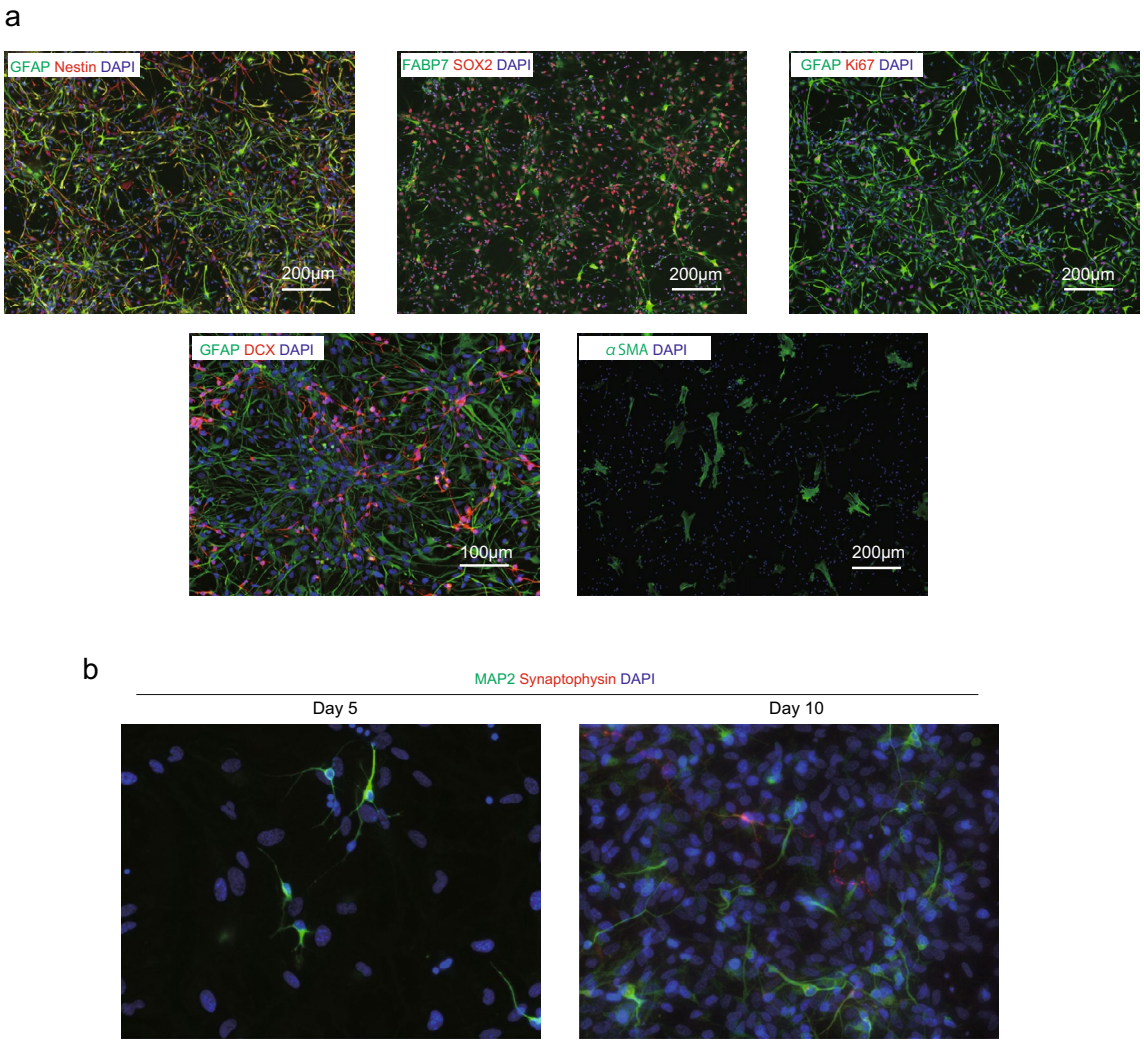

Fig. 5 Assessment of the cultured Ni-DPSCs. **a** Immunocytochemical staining of Ni-DPSCs at 2 DIV with antibodies against nestin, GAFP, SOX2, FABP7, Ki-67, DCX, and αSMA. **b** Immunocytochemical staining of Ni-DPSCs with antibodies against MAP2 and synaptophysin at 5 and 10 DIV

Briefly, during neurogenesis, neuroepithelial cells release nascent neurons and differentiate into radial glia. Radial glia differentiate asymmetrically and generate neurons through progenitor cells. Furthermore, they convert into astrocytes [38, 39]. In the trajectory inference and pseudotime analyses of Ni-DPSC differentiation, the neural progenitor cells first gave rise to neurons and then differentiated into astrocytes. This is similar to the course of in vivo neurodevelopment, and our neural induction method may be a suitable for generating neural progenitor cells similar to NSCs.

Neural induction of MSCs is mediated by epidermal growth factor, insulin, basic fibroblast growth factor, sonic hedgehog, nerve growth factor, and brain-derived neurotrophic factor, along with vitamin derivatives, such as retinoic acid and brain-derived neurotrophic factor [15, 40]. We focused not only on the factors mentioned above but also on hormone secretion during the formation of the neural plate, the original organ in the central nervous system. The neural plate begins to form when nutrient vessels from the placenta are not yet developed [41, 42]. The secretion of progesterone and estradiol from the early embryo, surrounding cumulus cells, and early placenta during this period is considered important for embryonic development and implantation [43–46]. Estrogen also induces a neural phenotype in ESCs and promotes the proliferation of embryonic NSCs as well as neuronal differentiation and maturation. [47, 48]. González-Orozco showed that progesterone plays an important role not only during pregnancy but also later in the development of the critical central nervous system [49]. Estradiol and progesterone in the neural induction medium used in this experiment may be important factors in inducing differentiation of MSCs into NSCs.

scRNA-seq revealed that non-neuronal cells were present in Ni-DPSCs, and in the trajectory and pseudotime analyses, astrocytes differentiated into non-neural lineage cells. However, it is unlikely that the beyond-embryonic differentiation of astrocytes into mesenchymal cells occurs. Pseudotime analysis of STREAM was performed on the assumption that the clusters are in the same differentiation pathway. It is likely that differentiation from astrocytes to non-neuronal cells was indicated. There are two possible explanations for the presence of non-neural lineage cells. Early neural rosettes derived from human ESCs contain a mixture of non-neuronal cells [50]. A neural rosette is a structure found during the neuronal induction of a universal cell—radially organized columnar epithelial cells with a lumen in the center that resembles the cross-section of a developing neural tube [8]. In addition, neural rosettes are capable of generating neurons and glia and serve as sites for the proliferation and maintenance of NSCs. Considering retrospective differentiation, our neural induction method may have produced cells with stem cell properties comparable with those of the early neural rosettes. Furthermore, the possibility of differentiation of a single cell must be considered. Kuroda et al. [51] identified cells with pluripotency in stromal cells and named them multilineage-differentiating stress-enduring (Muse) cells [51, 52]. Muse cells present in DPSCs may give rise to ectodermal neural lineages and mesodermal lineage cells. Neural crest lineage cells such as Schwann cells are partially mixed in NSCs induced from ESCs and iPSCs [53]. However, in this study, scRNA-seq did not reveal the presence of neural crest lineage cells.

This study had certain limitations. First, DPSCs were isolated by initially culturing dental pulp component cells at a sparse concentration and subsequently selecting the largest colonies as the DPSC colonies [2, 3, 22]. Consequently, the possibility that DPSC colonies did not form from a single cell cannot be excluded, indicating that progenitor cells of alternative cell types may have contaminated the cell culture. In addition, DPSCs represent a heterozygous cell population; nonetheless, the characteristics of the DPSCs used in the experiment were not stipulated. Although it is difficult for current technology to specifically stimulate individual cells with predetermined traits, differentiation and proliferation occur simultaneously. Future challenges lie in characterizing the DPSCs used in our experiments and ascertaining the DPSC characteristics most conducive to neural induction. In a previous study, we demonstrated the presence of platelet-derived growth factor alpha-positive oligodendrocyte progenitor cells at Ni-DPSCs [22]; however, in this study, we did not find oligodendrocyte-lineage cells differentiated from NSCs using scRNA-seq. Further evaluation is needed to determine whether this could have been due to a technical or analytical problem or was an individual difference.

In summary, our results revealed 13 clusters based on the expression of genes across the cell population, and five cell populations, namely neural progenitor cells, astrocytes, neurons, epithelial cells/smooth muscle cells, and fibroblasts/mesenchymal cells, were identified. Furthermore, pseudotime analysis showed that neural progenitor cells generated neurons, after which they differentiated into astrocytes. This study demonstrates the utility of scRNA-seq for the neural induction of MSCs. Ni-DPSCs could potentially be an alternative to pluripotent cells in cell-based therapies for neural diseases.

Supplementary Information The online version contains supplementary material available at https://doi.org/10.1007/s13577-024-01121-7.

Author contributions S. Takaoka: contributed to study conception and design, data acquisition and analysis, and manuscript drafting. F. Uchida: contributed to the study conception and design, data analysis, and drafting of the manuscript. H. Ishikawa, E Ishikawa, and H. Bukawa: contributed to the study conception and design, data analysis and interpretation, and drafting and critical revision of the manuscript. J. Toyomura, A. Ohyama, M. Hideaki, and K. Hirata: contributed to data acquisition, analysis, interpretation, and drafting of the manuscript. A. Marushima, K. Yamagata T. Yanagawa, and Y. Matsumaru: contributed to data interpretation and critical revision of the manuscript. N. Ishibashi-Kanno and S. Fukuzawa: contributed to data analysis and interpretation and critical revision of the manuscript. All the authors have approved the final version of the manuscript and agreed to be accountable for all aspects of the study.

Funding This work was supported in part by JSPS KAKENHI (Grant Number: JP22K21029, JP22K16035) to ST, and by JST FOREST Program (Grant Number: JPMJFR2112) to AM.

Data availability Data is provided within the manuscript and also available from the corresponding author upon a reasonable request.

Declarations

Conflict of interest The authors declare no potential conflicts of interest pertaining to the authorship and/or publication of this article.

Ethical approval This study was approved by the University of Tsukuba Clinical Research Ethics Review Committee (Approval Number: H29-173).

Informed consent Informed consent was received from the study participants.

References

1. Johansson CB, Momma S, Clarke DL, Risling M, Lendahl U, Frisén J. Identification of a neural stem cell in the adult mammalian central nervous system. Cell. 1999;96:25–34.
2. Hirata K, Marushima A, Nagasaki Y, et al. Efficacy of redox nanoparticles for improving survival of transplanted cells in a mouse model of ischemic stroke. Hum Cell. 2023;36:1703–15.
3. Matsumura H, Marushima A, Ishikawa H, et al. Induced neural cells from human dental pulp ameliorate functional recovery

in a murine model of cerebral infarction. Stem Cell Rev Rep. 2022;18:595–608.
4. Oyama H, Nukuda A, Ishihara S, Haga H. Soft surfaces promote astrocytic differentiation of mouse embryonic neural stem cells via dephosphorylation of MRLC in the absence of serum. Sci Rep. 2021;11:19574.
5. Zhao L, Liu JW, Shi HY, Ma YM. Neural stem cell therapy for brain disease. World J Stem Cells. 2021;13:1278–92.
6. Galiakberova AA, Dashinimaev EB. Neural stem cells and methods for their generation from induced pluripotent stem cells *in vitro*. Front Cell Dev Biol. 2020;8:815.
7. Chambers SM, Fasano CA, Papapetrou EP, Tomishima M, Sadelain M, Studer L. Highly efficient neural conversion of human ES and iPS cells by dual inhibition of SMAD signaling. Nat Biotechnol. 2009;27:275–80.
8. Fedorova V, Vanova T, Elrefae L, et al. Differentiation of neural rosettes from human pluripotent stem cells in vitro is sequentially regulated on a molecular level and accomplished by the mechanism reminiscent of secondary neurulation. Stem Cell Res. 2019;40: 101563.
9. Mariani J, Simonini MV, Palejev D, et al. Modeling human cortical development in vitro using induced pluripotent stem cells. Proc Natl Acad Sci U S A. 2012;109:12770–5.
10. Berryer MH, Tegtmeyer M, Binan L, et al. Robust induction of functional astrocytes using NGN 2 expression in human pluripotent stem cells. IScience. 2023;26:106995.
11. Meijer M, Rehbach K, Brunner JW, et al. A single-cell model for synaptic transmission and plasticity in human iPSC-derived neurons. Cell Rep. 2019;27:2199-211.e6.
12. Sloan SA, Darmanis S, Huber N, et al. Human astrocyte maturation captured in 3D cerebral cortical spheroids derived from pluripotent stem cells. Neuron. 2017;95:779-90.e6.
13. Pelegri NG, Milthorpe BK, Gorrie CA, Santos J. Neurogenic marker expression in differentiating human adipose derived adult mesenchymal stem cells. Stem Cell Investig. 2023;10:7.
14. Yi S, Cong Q, Zhu Y, Xu Q. Mechanisms of action of mesenchymal stem cells in metabolic-associated fatty liver disease. Stem Cells Int. 2023;2023:3919002.
15. Hernández R, Jiménez-Luna C, Perales-Adán J, Perazzoli G, Melguizo C, Prados J. Differentiation of human mesenchymal stem cells towards neuronal lineage: clinical trials in nervous system disorders. Biomol Ther (Seoul). 2020;28:34–44.
16. Chung CS, Fujita N, Kawahara N, Yui S, Nam E, Nishimura R. A comparison of neurosphere differentiation potential of canine bone marrow-derived mesenchymal stem cells and adipose-derived mesenchymal stem cells. J Vet Med Sci. 2013;75:879–86.
17. Khan AA, Huat TJ, Al Mutery A, et al. Significant transcriptomic changes are associated with differentiation of bone marrow-derived mesenchymal stem cells into neural progenitor-like cells in the presence of bFGF and EGF. Cell Biosci. 2020;10:126.
18. Sakai K, Yamamoto A, Matsubara K, et al. Human dental pulp-derived stem cells promote locomotor recovery after complete transection of the rat spinal cord by multiple neuro-regenerative mechanisms. J Clin Invest. 2012;122:80–90.
19. Gao Y, Tian Z, Liu Q, et al. Neuronal cell differentiation of human dental pulp stem cells on synthetic polymeric surfaces coated with ECM proteins. Front Cell Dev Biol. 2022;10: 893241.
20. Kogo Y, Seto C, Totani Y, et al. Rapid differentiation of human dental pulp stem cells to neuron-like cells by high K^+ stimulation. Biophys Physicobiol. 2020;17:132–9.
21. Luke AM, Patnaik R, Kuriadom S, Abu-Fanas S, Mathew S, Shetty KP. Human dental pulp stem cells differentiation to neural cells, osteocytes and adipocytes-An *in vitro* study. Heliyon. 2020;6:e03054 (**Erratum in: Heliyon. 2020;6:e03308**).
22. Takaoka S, Uchida F, Ishikawa H, et al. Transplanted neural lineage cells derived from dental pulp stem cells promote peripheral nerve regeneration. Hum Cell. 2022;35:462–71.
23. Takahashi H, Ishikawa H, Tanaka A. Regenerative medicine for Parkinson's disease using differentiated nerve cells derived from human buccal fat pad stem cells. Hum Cell. 2017;30:60–71.
24. Killoy KM, Harlan BA, Pehar M, Vargas MR. FABP7 upregulation induces a neurotoxic phenotype in astrocytes. Glia. 2020;68:2693–704.
25. Gerstner JR, Perron IJ, Riedy SM, et al. Normal sleep requires the astrocyte brain-type fatty acid binding protein FABP7. Sci Adv. 2017;3: e1602663.
26. Aruga J, Tohmonda T, Homma S, Mikoshiba K. Zic1 promotes the expansion of dorsal neural progenitors in spinal cord by inhibiting neuronal differentiation. Dev Biol. 2002;244:329–41.
27. Inoue T, Ota M, Ogawa M, Mikoshiba K, Aruga J. Zic1 and Zic3 regulate medial forebrain development through expansion of neuronal progenitors. J Neurosci. 2007;27:5461–73.
28. Gao S, Guo X, Zhao S, et al. Differentiation of human adipose-derived stem cells into neuron/motoneuron-like cells for cell replacement therapy of spinal cord injury. Cell Death Dis. 2019;10:597.
29. Bai WF, Zhang Y, Xu W, et al. Isolation and characterization of neural progenitor cells from bone marrow in cell replacement therapy of brain injury. Front Cell Neurosci. 2020;14:49.
30. Bueno C, Martínez-Morga M, García-Bernal D, Moraleda JM, Martínez S. Differentiation of human adult-derived stem cells towards a neural lineage involves a dedifferentiation event prior to differentiation to neural phenotypes. Sci Rep. 2021;11:12034.
31. Fu L, Zhu L, Huang Y, Lee TD, Forman SJ, Shih CC. Derivation of neural stem cells from mesenchymal stem cells: Evidence for a bipotential stem cell population. Stem Cells Dev. 2008;17:1109–21.
32. Urrutia DN, Caviedes P, Mardones R, Minguell JJ, Vega-Letter AM, Jofre CM. Comparative study of the neural differentiation capacity of mesenchymal stromal cells from different tissue sources: an approach for their use in neural regeneration therapies. PLoS ONE. 2019;14: e0213032.
33. Karakaş N, Bay S, Türkel N, et al. Neurons from human mesenchymal stem cells display both spontaneous and stimuli responsive activity. PLoS ONE. 2020;15: e0228510.
34. Brown C, McKee C, Halassy S, Kojan S, Feinstein DL, Chaudhry GR. Neural stem cells derived from primitive mesenchymal stem cells reversed disease symptoms and promoted neurogenesis in an experimental autoimmune encephalomyelitis mouse model of multiple sclerosis. Stem Cell Res Ther. 2021;12:499.
35. Heubach JF, Graf EM, Leutheuser J, et al. Electrophysiological properties of human mesenchymal stem cells. J Physiol. 2004;554:659–72.
36. Gancheva MR, Kremer K, Breen J, et al. Effect of octamer-binding transcription factor 4 overexpression on the neural induction of human dental pulp stem cells. Stem Cell Rev Rep. 2024;20:797–815.
37. Jovic D, Liang X, Zeng H, Lin L, Xu F, Luo Y. Single-cell RNA sequencing technologies and applications: a brief overview. Clin Transl Med. 2022;12: e694.
38. Kriegstein A, Alvarez-Buylla A. The glial nature of embryonic and adult neural stem cells. Annu Rev Neurosci. 2009;32:149–84.
39. Liu DD, He JQ, Sinha R, et al. Purification and characterization of human neural stem and progenitor cells. Cell. 2023;186:1179-94.e15.
40. Woodbury D, Schwarz EJ, Prockop DJ, Black IB. Adult rat and human bone marrow stromal cells differentiate into neurons. J Neurosci Res. 2000;61:364–70.
41. Greene ND, Copp AJ. Neural tube defects. Annu Rev Neurosci. 2014;37:221–42.

42. Burton GJ, Jauniaux E. Development of the human placenta and fetal heart: synergic or independent? Front Physiol. 2018;9:373.
43. Shutt DA, Lopata A. The secretion of hormones during the culture of human preimplantation embryos with corona cells. Fertil Steril. 1981;35:413–6.
44. Laufer N, DeCherney AH, Haseltine FP, Behrman HR. Steroid secretion by the human egg-corona-cumulus complex in culture. J Clin Endocrinol Metab. 1984;58:1153–7.
45. Punnonen R, Lukola A. Binding of estrogen and progestin in the human fallopian tube. Fertil Steril. 1981;36:610–4.
46. Tal R, et al. Taylor HS 2021 Endocrinology of pregnancy. In: Feingold KR, Anawalt B, Blackman MR, et al., editors. Endotext [Internet]. South Dartmouth (MA): MDText.com, Inc.; 2000. (**PMID: 25905197**).
47. Ray R, Novotny NM, Crisostomo PR, Lahm T, Abarbanell A, Meldrum DR. Sex steroids and stem cell function. Mol Med. 2008;14:493–501.
48. Bukovsky A, Caudle MR, Svetlikova M. Steroid-mediated differentiation of neural/neuronal cells from epithelial ovarian precursors in vitro. Cell Cycle. 2008;7:3577–83.
49. Pluchino N, Russo M, Genazzani AR. The fetal brain: role of progesterone and allopregnanolone. Horm Mol Biol Clin Investig. 2016;27:29-34X.
50. Elkabetz Y, Panagiotakos G, Al Shamy G, Socci ND, Tabar V, Studer L. Human ES cell-derived neural rosettes reveal a functionally distinct early neural stem cell stage. Genes Dev. 2008;22:152–65 (**Erratum in: Genes Dev. 2008;22:1257**).
51. Kuroda Y, Kitada M, Wakao S, et al. Unique multipotent cells in adult human mesenchymal cell populations. Proc Natl Acad Sci U S A. 2010;107:8639–43.
52. Dezawa M. Muse cells provide the pluripotency of mesenchymal stem cells: direct contribution of muse cells to tissue regeneration. Cell Transplant. 2016;25:849–61.
53. Pruszak J, Ludwig W, Blak A, Alavian K, Isacson O. CD15, CD24, and CD29 define a surface biomarker code for neural lineage differentiation of stem cells. Stem Cells. 2009;27:2928–40.